Published in final edited form as:
Acta Biomater. 2012 January ; 8(1): 415–423. doi:10.1016/j.actbio.2011.07.034.

Porous and strong bioactive glass (13–93) scaffolds prepared by unidirectional freezing of camphene-based suspensions

Xin Liu[1], **Mohamed N. Rahaman**[1,*], **Qiang Fu**[2], and **Antoni P. Tomsia**[2]

[1]Department of Materials Science and Engineering and Center for Bone and Tissue Repair and Regeneration, Missouri University of Science and Technology, Rolla, MO 65409, USA

[2]Materials Sciences Division, Lawrence Berkeley National Laboratory, Berkeley, CA 94720, USA

Abstract

Scaffolds of 13–93 bioactive glass ($6Na_2O$, $12K_2O$, 5MgO, 20CaO, $4P_2O_5$, $53SiO_2$; wt %) with an oriented pore architecture were formed by unidirectional freezing of camphene-based suspensions, followed by thermal annealing of the frozen constructs to grow the camphene crystals. After sublimation of the camphene, the constructs were sintered (1 h at 700 °C) to produce a dense glass phase with oriented macropores. The objective of this work was to study how constant freezing rates (1–7 °C/min) during the freezing step influenced the pore orientation and mechanical response of the scaffolds. When compared to scaffolds prepared by freezing the suspensions on a substrate kept at a constant temperature of 3 °C (time-dependent freezing rate), higher freezing rates resulted in better pore orientation, a more homogeneous microstructure, and a marked improvement in the mechanical response of the scaffolds in compression. Scaffolds fabricated using a constant freezing rate of 7 °C/min (porosity = 50 ± 4%; average pore diameter = 100 μm), had a compressive strength of 47 ± 5 MPa and an elastic modulus of 11 ± 3 GPa (in the orientation direction). In comparison, scaffolds prepared by freezing on the constant-temperature substrate had strength and modulus values of 35 ± 11 MPa and 8 ± 3 GPa, respectively. These oriented bioactive glass scaffolds prepared by the constant freezing rate route could potentially be used for the repair of defects in load-bearing bones, such as segmental defects in the long bones.

Keywords

bioactive glass; scaffold; unidirectional freezing; camphene; bone repair

1. Introduction

There is a need to develop new scaffolds to repair large defects in load-bearing bones using materials that are biocompatible and durable during the patient's lifetime [1]. Treatment methods based on the use of bone autografts and allografts are effective for the repair of contained defects in non-loaded bone which do not require a significant amount of graft material. However, they suffer from limitations (e.g., donor site morbidity; limited supply; possible transmission of diseases; high costs). Synthetic biocompatible scaffolds that replicate the structure and function of bone would be ideal bone substitutes, provided they

*Corresponding author: Tel.: 1-573-341-4406; fax: 1-573-341-6934, rahaman@mst.edu (M. N. Rahaman).

have the requisite mechanical properties for reliable long-term cyclical loading during weight bearing.

Scaffolds should have a porous microstructure suitable for supporting tissue ingrowth, and mechanical properties comparable to those of the tissue to be replaced. An interconnected pore size (diameter or width of the openings between adjoining pores) of 100 μm is considered to be the minimum requirement to permit tissue ingrowth and function [2]. The repair of segmental defects in load-bearing bones such as the long bones often involves the substitution of defects larger than a few centimeters [3]. Therefore it is essential that processing methods provide control of the microstructure over the entire dimensions of the scaffold in order to achieve the requisite mechanical reliability of the scaffold.

The mechanical response of porous materials with an anisotropic microstructure is strongly dependent on the pore orientation [4–6]. Commonly, the mechanical response in the pore orientation direction is often far superior to that in the perpendicular direction, and superior to that for scaffolds with a random microstructure. For example, the compressive strength and elastic modulus of human cortical bone in the orientation direction are almost twice those in the perpendicular direction [7]. The formation of scaffolds with oriented pore architectures could provide an approach for creating porous and strong three-dimensional (3D) scaffolds for applications in the repair of loaded bone.

Unidirectional freezing of aqueous suspensions has been used recently to produce oriented scaffolds of bioceramics and bioactive glass [8, 9]. The process commonly results in the formation of porous constructs with a lamellar microstructure. However, the width of the slot-like pores (10–40 μm) is considered to be too small to support tissue ingrowth. A variety of techniques has been used to control the width and morphology of the pores, such as the use of different freezing rates [10], modification of the solvent composition [11–13], patterning of the cold substrate [14], application of an electric field [15], and coarsening of the crystals [16]. In addition, control of the freezing rate has been shown to lower the variation in the pore width along the freezing direction [17, 18], and to provide a homogenous lamellar microstructure over several centimeters [19]. However, in addition to the narrow pore width of the scaffolds mentioned above, another limitation in the use of aqueous solvents is the chemical degradation of the bioactive glass, particularly for more reactive borosilicate and borate bioactive glasses.

Our previous work showed that the use of organic (camphene)-based suspensions, coupled with a two-step forming process, can alleviate the above-mentioned limitations of aqueous suspensions [16]. Bioactive glass scaffolds prepared from camphene-based suspensions had a columnar microstructure with average pore diameters larger than 100 μm. The two-step process consisted of unidirectional freezing of the suspension on a substrate kept at a constant temperature (3 °C) followed by thermal annealing, typically for ~24 h at ~35 °C (near the softening point of the frozen mixture). In the freezing step, solid camphene dendrites form in the suspension of bioactive glass particles in liquid camphene, starting at the interface with the cold substrate and growing down the temperature gradient (Fig. 1). The dendrites redistribute the particles, which are concentrated in the inter-dendritic spaces. The result is a frozen construct consisting of particle-free solid dendrites and inter-dendritic material of bioactive glass particles in fine-scale frozen camphene. Upon sublimation of the camphene, the primary dendrites become macropores which are separated by concentrated glass particulate regions in the shape of the inter-dendritic spaces. Sintering results in the preferential removal of the fine pores in the particulate regions, giving a cellular scaffold with dense glass struts approximating the shape of the inter-dendritic regions and macropores in the shape of the primary dendrites. Annealing the frozen construct near the solidification temperature of the suspension leads to coarsening of the primary dendrites and

removal of the secondary dendrite arms. As a result, the annealed construct has uniaxially-aligned primary dendrites with larger diameter than the frozen construct, which are better for long bone scaffolds.

In our previous work [16], unidirectional freezing on a constant-temperature substrate did not provide a constant freezing rate. Instead, the freezing rate was time-dependent, decreasing with time as the solidification front moved from the cold substrate to the top of the sample. Because of this time-dependent freezing rate, the achievement of uniaxially-aligned camphene dendrites and homogeneity of the dendrite diameter was limited to only ~1 cm.

In the present work, an apparatus was assembled to study unidirectional freezing of camphene-based suspensions at constant freezing rates. We hypothesized that the use of constant freezing rates could create constructs with more spatially uniform dendrites, resulting in the production of bioactive glass scaffolds with improved mechanical properties (in the orientation direction). Constructs of silicate 13–93 glass were formed using the two-step freezing and annealing process described previously. In the freezing step, constant freezing rates in the range 1–7 °C/min were used. The effect of the freezing rate on the pore orientation, microstructural homogeneity, and mechanical response of the fabricated scaffolds was studied. For comparison, scaffolds were prepared using the same process but with the freezing step carried out on a substrate held at a constant temperature, as described in our previous work [16].

Silicate 13–93 bioactive glass was used in this work because of our previous experience with forming scaffolds of this glass using other techniques [9, 20–22]. In addition, 13–93 bioactive glass has better processing characteristics by viscous flow sintering than the more widely researched 45S5 glass. While it is based on the 45S5 composition, 13–93 glass has a higher SiO_2 content, plus additional network modifiers, such as K_2O and MgO [23], which provides a larger window between the glass transition temperature and the onset of crystallization. As a result, the glass phase in porous constructs formed from 13–93 glass particles can be sintered to high density without crystallization, which often leads to an improvement in the mechanical strength of the scaffolds. Furthermore, in vitro cell culture showed no marked difference between the ability of 13–93 and 45S5 glass to support the proliferation and function of osteoblastic cells [24].

2. Materials and methods

2.1 Preparation of oriented 13–93 bioactive glass scaffolds

The fabrication of bioactive glass (13–93) scaffolds with oriented pores by unidirectional freezing of camphene-based suspensions was performed using a sequence of steps [16]: preparation of a homogeneous suspension; unidirectional freezing of the suspension; isothermal annealing of the frozen constructs near the softening point of the mixture to coarsen the camphene crystals; sublimation of the camphene crystals to replicate the macropores; and sintering to densify the glass phase in the macropore walls.

The procedure for preparing camphene-based suspensions is described in detail elsewhere [16]. Briefly, bioactive glass with the 13–93 composition ($6Na_2O$, $12K_2O$, 5MgO, 20CaO, $4P_2O_5$, $53SiO_2$; wt %) (kindly provided by Mo-Sci Corp., Rolla, Missouri), was ground to produce particles with an average size of ~1 μm. Suspensions were prepared by ball milling a mixture of the glass particles (10 vol%), camphene ($C_{10}H_{16}$; CAS 5794-04-7; Alfa Aesar, Ward Hill, MA, USA), and 2 wt% of isostearic acid ($C_{18}H_{36}O_2$; MP Biomedicals LLC, Solon, OH, USA) for 24 h at 55 °C in a closed polypropylene bottle.

Unidirectional freezing of the suspensions was performed at selected constant freezing rates in the range 1–7 °C/min using a specially assembled apparatus, described in detail elsewhere [25]. Briefly, the suspension was poured into a polytetrafluoroethylene (PTFE) mold which was surrounded by a heating jacket and placed on a cold copper rod (cold finger). Since camphene could freeze at room temperature, a constant output was applied to the heating jacket which kept the mold temperature at around 35 °C in order to minimize the heat transfer through the mold. The mold was also covered with a rubber cap to prevent heat transfer from the top. The cold finger was cooled by liquid nitrogen. The temperature of the cold finger was controlled by another heating jacket, a thermocouple within the cold finger, and a proportional–integral–derivative (PID) controller. Frozen constructs with a diameter of ~10 mm and a length of ~20 mm were prepared. For comparison, unidirectional freezing was also performed by freezing the suspensions on a copper substrate kept at a constant temperature of 3 °C, as described in our previous work [16].

After freezing, each construct was placed in a closed poly(vinyl chloride) (PVC) container to avoid camphene loss, and annealed for 24 h at 34 °C in an incubator to coarsen the camphene dendrites. The samples were cooled to room temperature, removed from the PVC containers, and kept for 24 h at room temperature in a fume hood to sublime the camphene phase. Finally, the porous constructs were sintered in air for 1 h at 700 °C (heating rate = 5°C/min) to remove the fine pores between the bioactive glass particles in the walls of the oriented macropores.

2.2 Microstructural characterization of porous constructs

After sublimation of the camphene, the porous constructs were pre-sintered (5 h at 600 °C) in order to develop adequate strength for handling but to maintain the as-formed porous microstructure. These pre-sintered constructs were sectioned in planes parallel and perpendicular to the freezing direction, infiltrated with epoxy resin, ground and polished. The polished sections were coated with Au/Pd, and examined in a scanning electron microscopy, SEM (S-4700; Hitachi, Tokyo, Japan) at an accelerating voltage of 15 kV and a working distance of 18 mm. Sections of the sintered constructs (1 h at 700 °C) were also prepared and examined using a similar procedure.

The line intercept method was used to determine the average pore diameter of the constructs from sections perpendicular to the freezing direction. More than 100 intersections were counted. The open porosity of the sintered constructs was measured using the Archimedes method. The pore size distribution was determined using a liquid extrusion porosimeter (LEP-1100 AX, Porous Materials Inc., NY), with water used as the wetting liquid.

2.3 Mechanical response of sintered scaffolds

The mechanical response of the sintered constructs in the direction of freezing was measured in compression using an Instron testing machine (Model 4204; Norwood, MA, USA). Cylindrical constructs (7 mm in diameter × 7 mm) were deformed at a rate of 0.5 mm/min. Six samples were tested for each group, and the compressive strength and elastic modulus were determined as an average ± standard deviation. Statistical analysis was performed using one-way ANOVA. After testing, the fractured surfaces of the scaffolds were examined using SEM.

3. Results

3.1 Freezing rate of suspensions

Figure 2 shows the temperature of the cold finger (copper rod) as a function of time for the freezing process at three different freezing rates (1, 4, and 7 °C/min). Higher cooling rates

were limited by the conductivity and the lowest achievable temperature of the copper rod. In order to maintain the required freezing rate, the temperature of the copper rod was lowered continuously with the aid of the PID controller. The average solidification rates, 4, 10, and 16 μm/s, for the freezing rates of 1, 4, and 7 °C/min, respectively, were determined from the length of the frozen construct and the time required to completely freeze the construct. For comparison, the time for complete freezing is also shown for the suspensions frozen on the constant-temperature substrate (3 °C).

3.2 Microstructure of frozen constructs

Figure 3 shows SEM images of the cross-sections parallel to the freezing direction for constructs prepared at constant freezing rates of 1 and 7 °C/min, after sublimation of the camphene; for comparison, SEM images of constructs prepared by freezing on a constant-temperature substrate (3 °C) are also shown. Images for constructs frozen at 4 °C/min are not shown for the sake of brevity. The images were taken at the top, middle, and bottom region along the length of the construct. Generally, the pores showed a dendritic morphology, resulting from the growth of primary camphene dendrites down the imposed temperature gradient, and side-branching or secondary camphene dendrites emanating from the primary dendrites. However, the spatial homogeneity of the pore diameter was dependent on the freezing method and the rate of freezing.

The constructs frozen on the constant-temperature substrate (Figs. 3A1-A3) had a vastly different microstructure from bottom to top. Starting with fine oriented pores at the bottom of the construct, the diameter of the pores increased markedly with distance along the freezing direction. For the constructs frozen at constant rates, the lowest rate (1 °C/min) resulted in an improvement in the homogeneity of the pore diameter between the bottom and top of the construct (Figs. 3B1–B3). The spatial homogeneity of the pore diameter continued to increase with increasing freezing rate, until at the highest rate used (7 °C/min), there was little difference in the homogeneity of the pore diameter from the bottom to the top of the construct, a length of ~20 mm (Figs. 3C1–C3).

Using the cross sections perpendicular to the freezing direction, the average pore diameter was determined at the bottom, middle, and top regions of the constructs (Fig. 4a). As shown, there were significant differences in pore diameter between the three regions for all the constructs except for those frozen at the highest rate of 7 °C/min, for which there was a significant difference between the middle and top regions only. The average pore diameter, normalized to the pore diameter at the bottom of the construct, is shown in Fig. 4b as a function of distance from the bottom of the construct. For the construct frozen on the constant-temperature substrate (3 °C), the average pore diameter at the top was ~3 times the value at the bottom. In comparison, for the construct prepared by freezing at a constant rate of 7 °C/min, the difference in average pore size along the length was markedly smaller.

3.3 Microstructure of constructs after annealing and sintering

SEM images of the cross-sections parallel to freezing direction are shown in Fig. 5 for the constructs after the freezing and thermal annealing (24 h at 34 °C) steps, and after sublimation of the camphene. The images are shown for the bottom, middle, and top regions of the samples frozen on the constant-temperature substrate (3 °C) and under constant freezing rates of 7 °C/min. When compared to the microstructures of the constructs after the freezing step only (no thermal annealing) (Fig. 3), the diameter of the pores resulting from the primary camphene dendrites has increased markedly. There is also an absence of pores from the secondary dendrite arms in the construct frozen at 7 °C/min (Figs. 5B1–B3). In the case of the constructs frozen on the constant-temperature substrate, the absence of pores from the secondary dendrite arms is not clearly evident (Figs. 5A1–5A3).

In general, the orientation of the pores was more evident after the annealing step, and the average pore diameter showed little dependence on the freezing rates used in this work. However, there was some difference in the pore morphology. The constructs prepared by freezing on the constant-temperature substrate showed some difference in the thickness of the macropore walls from the bottom to the top of the construct (Figs. 5A1–5A3). For this group, no clear orientation of the pores was observed at the top of the constructs. In comparison, the constructs frozen at constant rates showed better homogeneity in the thickness of the struts (macropore walls) and the pore diameter along the length of the construct. Constructs frozen under the fastest rate (7°C/min) showed well-aligned pores along the freezing direction, and channel-like pores can be observed along the freezing direction (Figs. 5B1–5B3).

After sintering, the scaffolds had approximately the same porosity of 50 ± 4%, regardless of the conditions used in the freezing step. For the scaffolds prepared by freezing on the constant-temperature substrate (3 °C), SEM images of the cross sections parallel to the freezing direction showed differences in pore alignment along the length of the construct (Fig. 6a). The pores were well oriented from the bottom to the middle of the scaffolds, but were poorly aligned above the middle region. In comparison, the constructs prepared by freezing at a constant rate of 7 °C/min showed good pore alignment and a homogeneous microstructure from the bottom to the top of the construct (Fig. 6b). SEM images of sections perpendicular to the freezing direction showed macropores with an approximately circular cross section (Figs. 6c, d) and almost fully dense glass struts (Fig. 6e).

The distributions of pore diameters for the sintered constructs formed by freezing on the constant-temperature substrate and under constant freezing rates of 1 °C/min and 7 °C/min are shown in Fig. 7. For all three groups, the pore sizes were mostly in the range 50–150 μm, with a peak value of ~100 μm. For the construct prepared by freezing at 7 °C/min, the pore size data followed an approximately bell-shaped curve, typical of a normal distribution. However, the data for the constructs prepared by freezing on the constant-temperature substrate or freezing at 1 °C/min showed a tail in the distribution curve at pore sizes larger than ~150 μm.

3.4. Mechanical response of sintered constructs

Figure 8a shows examples of the stress vs. deformation response in compression for the sintered constructs formed by freezing on the constant-temperature substrate (3 °C) and under a constant freezing rate of 7 °C/min. Both constructs showed an elastic response, in which the stress increased approximately linearly with deformation, followed by failure in which the samples fractured into several pieces, typical of dense brittle solids. The fracture planes were almost vertical, along the orientation direction; mirror area and hackle lines were found on the fractured surfaces of the glass struts, which are common features accompanying the failure of a dense glass. As shown in Fig. 8a, the construct formed by freezing at a constant rate had a higher compressive strength (stress at failure) than the construct formed by freezing on the constant-temperature substrate.

The compressive strength and elastic modulus (slope of the stress vs. deformation response) of the sintered constructs are shown in Fig. 8b. Constructs formed by freezing at the lowest rate (1 °C/min) had a compressive strength (37 ± 7 MPa) and an elastic modulus (8 ± 3 GPa) (data not shown) that were not significantly different from those for the construct formed by freezing on the constant-temperature substrate (strength = 35 ± 11 MPa; elastic modulus = 8 ± 3 GPa). In comparison, the construct formed by freezing at the highest rate (7 °C/min) had a significantly higher compressive strength (47 ± 5 MPa) ($p<0.05$) and a higher elastic modulus (11 ± 3 GPa) ($p<0.08$).

4. Discussion

The results of the present work show that controlled unidirectional freezing of camphene-based suspensions, under an imposed constant freezing rate, resulted in the formation of 13–93 bioactive glass constructs with a more homogeneous microstructure and better pore alignment, when compared to constructs formed under a time-dependent freezing rate (freezing on a constant-temperature substrate). The microstructural improvement resulted in an enhancement of the compressive strength and elastic modulus of the sintered constructs. Bioactive glass scaffolds (porosity = 50 ± 4%; average pore width ≈ 100 μm) formed by freezing at a constant rate of 7 °C/min (the highest freezing rate available in this work) showed a compressive strength of 47 ± 5 MPa and an elastic modulus of 11 ± 3 GPa. These scaffolds could have potential application in the repair of load-bearing bones, such as segmental defects in the long bones.

The results showed that after the freezing step, the homogeneity of the primary dendrite diameter over the length of the frozen construct was dependent on the method of freezing and the freezing rate (Figs. 3, 4). As described previously, freezing at constant rates of 1, 4, and 7 °C/min resulted in average solidification rates of approximately 4, 10, and 16 μm/s, respectively (Fig. 2). Therefore, the results showed that the spatial homogeneity of the dendrite diameters improved with increasing values of the solidification rate. In contrast, the solidification rate decreased with time for the constructs frozen on the constant-temperature substrate, resulting in a reduction in the homogeneity of the primary dendrite diameter over the length of the construct. In the present work, homogeneity of the camphene dendrite diameter was achieved over a sample length of ~30 mm for the highest solidification rate (16 μm/s) achievable with the equipment. In contrast, for constructs prepared by freezing on the constant temperature substrate (3 °C), homogeneity of the dendrite diameter was achieved over a distance of only ~10 mm.

The results (Figs. 3, 4) also showed a dependence of the diameter of the primary camphene dendrite on the solidification rate. Based on previous studies [8, 11, 19, 25, 26], the dependence of the average dendrite diameter d on the average solidification rate v was assumed to follow a power law relation

$$d = kv^{-m} \quad (1)$$

where k is a constant and m is an exponent. A plot of the data for d (taken from Fig. 4a) vs. v (taken from Fig. 2) showed that the exponent m varied from ~0.3 for the bottom region of the construct to ~0.6 for the top region (Fig. 9).

The pore channel size (width or diameter) in constructs prepared by the unidirectional freezing of suspensions has been found to depend on factors such as the solidification rate, the solvent, and the particles in the suspension. For suspensions of Al_2O_3 particles in camphene, Shanti et al. [26] did not measure the solidification rate directly, but assumed that the rate varied inversely with distance from the cold substrate. They plotted the pore channel size as a function of the relative solidification rate and found that $m = 0.33$. In comparison, for aqueous Al_2O_3 suspensions, the results from Deville et al. [25] and Waschkies et al. [19] for the average pore channel spacing as a function of the solidification rate give $m \approx 0.9$ and $m \approx 0.8$, respectively. The data from Zhang et al. [11] for the average pore spacing of constructs formed from aqueous solutions of poly(vinyl alcohol) give $m \approx 0.6$. The m values in the present work fall within the range of values described above for previous studies. The reason for the increase in the m values (0.3–0.6) from the bottom to the top of the construct

(Fig. 9) is not clear. However, a possible reason might be a decrease in the solidification rate with distance from the cold substrate.

As described previously, interconnected pores with a diameter or width between neighboring pores of ~100 μm are considered to be the minimum requirement for supporting tissue ingrowth and function [2]. Our previous work on unidirectional freezing of camphene-based suspensions on a constant-temperature substrate showed that this minimum pore diameter can be achieved or exceeded by using a two-step process (freezing followed by thermal annealing) [16]. That study also showed that the annealing step resulted in coarsening of the primary camphene dendrites, typical of an Ostwald ripening process. As a consequence, despite large differences in the diameter of the primary camphene dendrites formed after the freezing step, the annealing step resulted in a self-similar distribution of dendrite diameters with approximately the same average diameter. That trend was also observed in the present work. Constructs prepared by freezing on a constant-temperature substrate and under constant freezing rates (1–7 °C/min) had approximately the same average primary dendrite diameter after the annealing process (Fig. 5). After sintering, the constructs had approximately the same average pore diameter, and the distribution of pore diameters approximated a bell-shaped curve (Fig. 7). However, the construct formed by freezing at a constant rate of 7 °C/min showed a narrower distribution of pore sizes, which could result from the better homogeneity of the primary dendrite diameter achieved in the freezing step. In comparison, for the sample frozen on a constant-temperature substrate (3 °C), differences in the orientation and morphology of the pores (or crystals) resulting from the freezing step remained after the annealing and sintering steps (Figs. 5, 6).

The mechanical strength of the constructs is determined by their microstructure. In the present work, the sintered constructs can be approximated by a uniaxial composite consisting dense glass struts and channel voids. In this case, the compressive strength and elastic modulus can be described by a rule of mixtures. However, off-axis pores will reduce the strength and modulus. As discussed previously, higher freezing rates lead to better alignment of the pores and to fewer off-axis void channels, resulting in a higher strength and modulus (Fig. 8).

The repair of defects in load-bearing bones is a challenging clinical problem. Bioactive glass scaffolds with a more random microstructure, prepared by methods such as sintering of particles or short fibers (porosity = 40–50%), as well as polymer foam replication and sol-gel processing (porosity = 75–90%), often have compressive strength and stiffness in the range of those reported for trabecular bone [20, 21, 27–29]. Consequently, they are limited to the repair of non-loaded bone. In comparison, 13–93 bioactive glass scaffolds with an oriented microstructure prepared recently by unidirectional freezing of suspensions (porosity = 50%; average pore width = 100 μm) have shown average compressive strength (25–35 MPa) and elastic modulus (5–10 GPa), values far higher than those reported for trabecular bone [9, 16]. More recently, bioactive glass scaffolds (13–93 or 6P53B) with a grid-like microstructure prepared by solid freeform fabrication methods (porosity = 50–60%; pore width = 200–500 μm) have shown a compressive strength (~140 MPa), comparable to the values reported for cortical bone [22, 30, 31]. Although the guidelines for the requisite mechanical properties of scaffolds intended for loaded bone repair are currently unclear, the present method could provide bioactive glass scaffolds with a favorable combination of mechanical strength and pore characteristics for potential applications in the repair of loaded bone. The ability of these oriented scaffolds to substitute for bone defects is currently being evaluated in vivo in animal models.

5. Conclusion

Silicate 13–93 bioactive glass scaffolds with an oriented pore architecture were formed using a two-step process consisting of unidirectional freezing of camphene-based suspensions followed by thermal annealing near the softening point of the frozen mixture. The pore orientation and homogeneity of the microstructure were dependent primarily on the freezing conditions, whereas the pore width was controlled by the annealing step. Higher freezing rate (7 °C/min) resulted in improved pore alignment and a more homogeneous microstructure over a larger length of the sample. Constructs frozen on a cold substrate or at constant freezing rates of 1–7 °C/min had approximately the same average pore width after the annealing step. After sintering, constructs prepared by freezing at 7 °C/min (porosity = 50%; pore width = 100 μm) had a compressive strength of 47 ± 5 MPa and an elastic modulus of 11 ± 3 GPa. These bioactive glass scaffolds have a favorable combination of strength, stiffness, and pore characteristics for potential application in the repair of loaded bone.

Acknowledgments

This work was supported by the U.S. Army Medical Research Acquisition Activity, under Contract No. W81XWH-08-1-0765, and by the National Institutes of Health, National Institute of Arthritis, Musculoskeletal and Skin Diseases (NIH/NIAMS), Grant No. 1R15AR056119-01. Q.F. and A.P.T. are grateful for the support from the National Institutes of Health, National Institute of Dental and Craniofacial Research (NIH/NIDCR), Grant No. 1R01DE015633. The authors would like to thank Dr. D. E. Day and Mo-Sci Corp, Rolla, Missouri, for providing the bioactive glass used in this work, and C. Gilbert for assistance with setting up the controlled freezing rate apparatus.

References

1. U.S. Census Bureau. Health and nutrition. U.S. Census Bureau statistical abstracts of the United States; Washington, DC: 2009. p. 117
2. Hulbert SF, Young FA, Mathews RS, Klawitter JJ, Talbert CD, Stelling FH. Potential of ceramic materials as permanently implantable skeletal prostheses. J Biomed Mater Res. 1970; 4:433–56. [PubMed: 5469185]
3. Reichert JC, Saifzadeh S, Wullschleger ME, Epari DR, Schütz MA, Duda GN, Schell H, et al. The challenge of establishing preclinical models for segmental bone defect research. Biomaterials. 2009; 30:2149–63. [PubMed: 19211141]
4. Ma PX, Zhang R. Microtubular architecture of biodegradable polymer scaffolds. J Biomed Mater Res. 2001; 56:469–77. [PubMed: 11400124]
5. Fu Q, Rahaman MN, Dogan F, Bal BS. Freeze casting of porous hydroxyapatite scaffolds. II. Sintering, microstructure, and mechanical behavior. J Biomed Mater Res B. 2008; 86:514–22.
6. Shanjani Y, Hu Y, Pilliar RM, Toyserkani E. Mechanical characteristics of solid-freeform-fabricated porous calcium polyphosphate structures with oriented stacked layers. Acta Biomater. 2011; 7:1788–96. [PubMed: 21185409]
7. Wirtz DC, Schiffers N, Pandorf T, Radermacher K, Weichert D, Forst R. Critical evaluation of known bone materials properties to realize anisotropic FE-simulation of the proximal femur. J Biomech. 2000; 33:1325–30. [PubMed: 10899344]
8. Deville S, Saiz E, Tomsia AP. Freeze casting of hydroxyapatite scaffolds for bone tissue engineering. Biomaterials. 2006; 27:5480–9. [PubMed: 16857254]
9. Fu Q, Rahaman MN, Brown RF, Bal BS. Preparation and *in vitro* evaluation of bioactive glass (13–93) scaffolds with oriented microstructures for repair and regeneration of load-bearing bones. J Biomed Mater Res A. 2010; 93:1380–90. [PubMed: 19911380]
10. Hu L, Wang CA, Huang Y, Sun C, Lu S, Hu Z. Control of pore channel size during freeze casting of porous YSZ ceramics with unidirectionally aligned channels using different freezing temperatures. J Euro Ceram Soc. 2010; 30:3389–96.

11. Zhang H, Hussain I, Brust M, Butler M, Rannard SP, Cooper AI. Aligned two- and three-dimensional structures by directional freezing of polymers and nanoparticles. Nat Mater. 2005; 4:787–93. [PubMed: 16184171]
12. Rahaman MN, Fu Q. Manipulation of porous bioceramics microstructures by freezing of suspensions containing binary mixtures of solvents. J Am Ceram Soc. 2008; 9:4137–40.
13. Araki K, Halloran JW. Room-temperature freeze casting for ceramics with nonaqueous sublimable vehicles in the naphthalene–camphor eutectic system. J Am Ceram Soc. 2004; 87:2014–9.
14. Munch E, Saiz E, Tomsia AP. Architectural control of freeze-cast ceramics through additives and templating. J Am Ceram Soc. 2009; 92:1534–9.
15. Tang YF, Zhao K, Wei JQ, Qin YS. Fabrication of aligned lamellar porous alumina using directional solidification of aqueous slurries with an applied electrostatic field. J Euro Ceram Soc. 2010; 30:1963–5.
16. Liu X, Rahaman MN, Fu Q. Oriented bioactive glass (13–93) scaffolds with controllable pore size by unidirectional freezing of camphene-based suspensions: Microstructure and mechanical response. Acta Biomater. 2011; 7:406–16. [PubMed: 20807594]
17. Schoof H, Apel J, Heschel I, Rau G. Control of pore structure and size in freeze-dried collagen sponges. J Biomed Mater Res B. 2001; 58:352–7.
18. O'Brien FJ, Harley BA, Yannas IV, Gibson L. Influence of freezing rate on pore structure in freeze-dried collagen-GAG scaffolds. Biomaterials. 2004; 25:1077–86. [PubMed: 14615173]
19. Waschkies T, Oberacker R, Hoffmann MJ. Control of lamellae spacing during freeze casting of ceramics using double-side cooling as a novel processing route. J Am Ceram Soc. 2009; 92:S79–84.
20. Fu Q, Rahaman MN, Huang W, Day DE, Bal BS. Preparation and bioactive characteristics of a porous 13–93 Glass, and its fabrication into the articulating surface of a proximal tibia. J Biomed Mater Res A. 2007; 82:222–9. [PubMed: 17266021]
21. Fu Q, Rahaman MN, Bal BS, Brown RF, Day DE. Mechanical and *in vitro* performance of 13–93 bioactive glass scaffolds prepared by a polymer foam replication technique. Acta Biomater. 2008; 4:1854–64. [PubMed: 18519173]
22. Huang TS, Doiphode ND, Rahaman MN, Leu MC, Bal BS, Day DE. Porous and strong bioactive glass (13–93) scaffolds prepared by freeze extrusion fabrication. Mater Sci Eng C. 201110.1016/j.msec.2011.06.004
23. Brink M. The influence of alkali and alkaline earths on the working range for bioactive glasses. J Biomed Mater Res. 1997; 36:109–17. [PubMed: 9212395]
24. Brown RF, Day DE, Day TE, Jung S, Rahaman MN, Fu Q. Growth and differentiation of osteoblastic cells on 13–93 bioactive glass fibers and scaffolds. Acta Biomater. 2008; 4:387–396. [PubMed: 17768097]
25. Deville S, Saiz E, Nalla RK, Tomsia AP. Freezing as a path to build complex composites. Science. 2006; 311:515–518. [PubMed: 16439659]
26. Shanti NO, Araki K, Halloran JW. Particle redistribution during dendritic solidification of particle suspensions. J Am Ceram Soc. 2006; 89:2444–7.
27. Rahaman MN, Day DE, Brown RF, Fu Q, Jung SB. Nanostructured bioactive glass scaffolds for bone repair. Ceram Eng Sci Proc. 2008; 29:211–25.
28. Liu X, Huang W, Fu H, Yao A, Wang D, Pan H, Lu WW. Bioactive borosilicate glass scaffolds: improvement on the strength of glass-based scaffolds for tissue engineering. J Mater Sci: Mater Med. 2009; 20:365–72. [PubMed: 18807266]
29. Jones JR, Ehrenfried LM, Hench LL. Optimising bioactive glass scaffolds for bone tissue engineering. Biomaterials. 2006; 27:964–73. [PubMed: 16102812]
30. Doiphode ND, Huang TS, Leu MC, Rahaman MN, Day DE. Freeze extrusion fabrication of 13–93 bioactive glass scaffolds for bone repair. J Mater Sci: Mater Med. 2011; 22:515–23. [PubMed: 21279671]
31. Fu Q, Saiz E, Tomsia AP. Bio-inspired highly porous and strong glass scaffolds. Adv Funct Mater. 2010; 21:1058–63. [PubMed: 21544222]

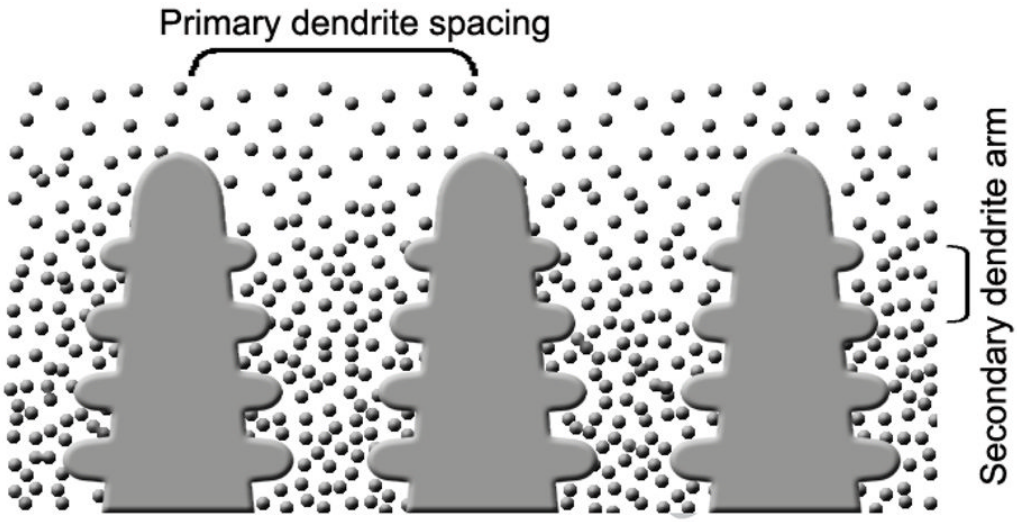

Fig. 1.
Schematic of the growth of camphene dendrites during unidirectional freezing of camphene-based suspensions [16].

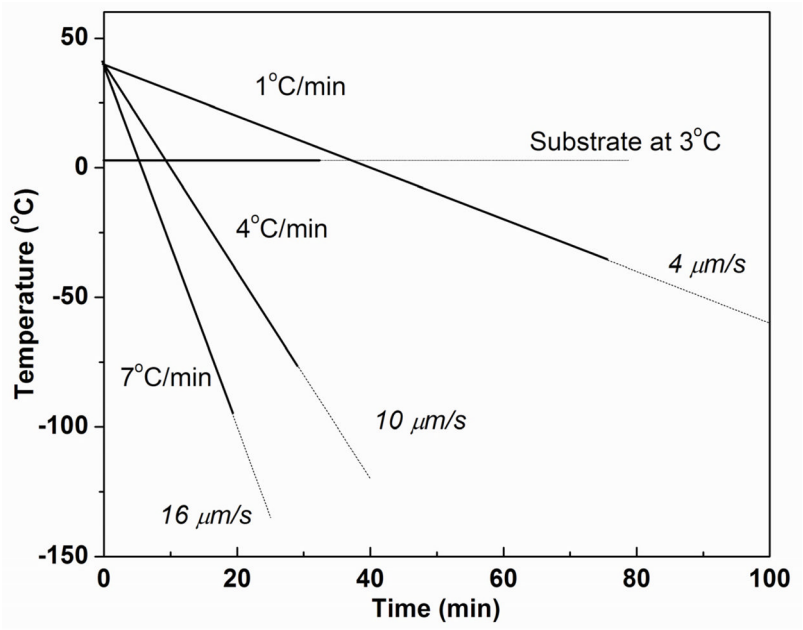

Fig. 2.

Data for the **s**ubstrate (cold finger) temperature vs. time during unidirectional freezing of camphene-based suspensions at constant rates (1–7 °C/min). The average velocity of the camphene solidification front is shown for each freezing rate. For comparison, suspensions were also frozen on a substrate kept at a constant temperature (3 °C). The solid lines show the time taken to completely freeze a construct 20 mm in height under the conditions shown.

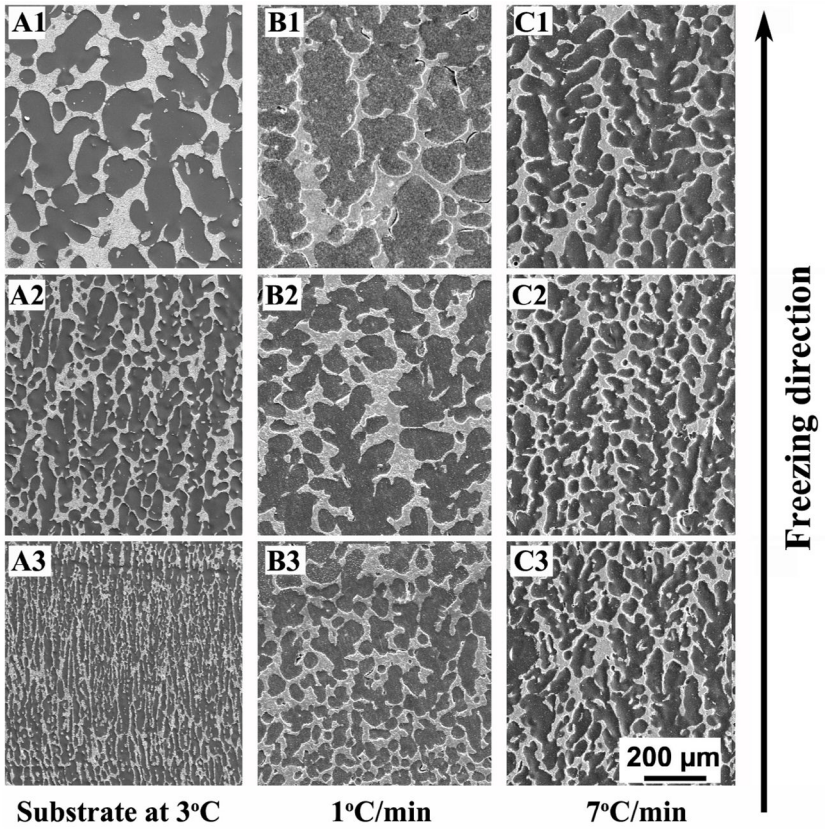

Fig 3.

SEM images of the cross-sections parallel to the freezing direction for as-solidified 13–93 bioactive glass constructs prepared by unidirectional freezing on a constant-temperature substrate (3°C) (A1–A3), or at constant freezing rates of 1 °C/min (B1–B3), and 7°C/min(C1–C3). Images are shown for the bottom, middle, and top portions of the constructs along the freezing direction.

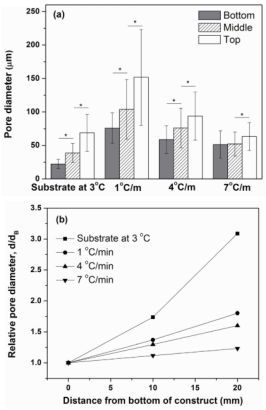

Fig. 4.

(a) Pore diameter at the bottom, middle, and top portions of the construct after the freezing step and sublimation of the camphene, for constructs frozen unidirectionally on a constant-temperature substrate (3 °C) or at constant rates (1, 4, and 7 °C/min) (*$p < 0.05$); (b) Pore diameter (normalized to the pore diameter at the bottom portion of the construct) vs. distance from the bottom of the construct plotted from the data in Fig. 4a.

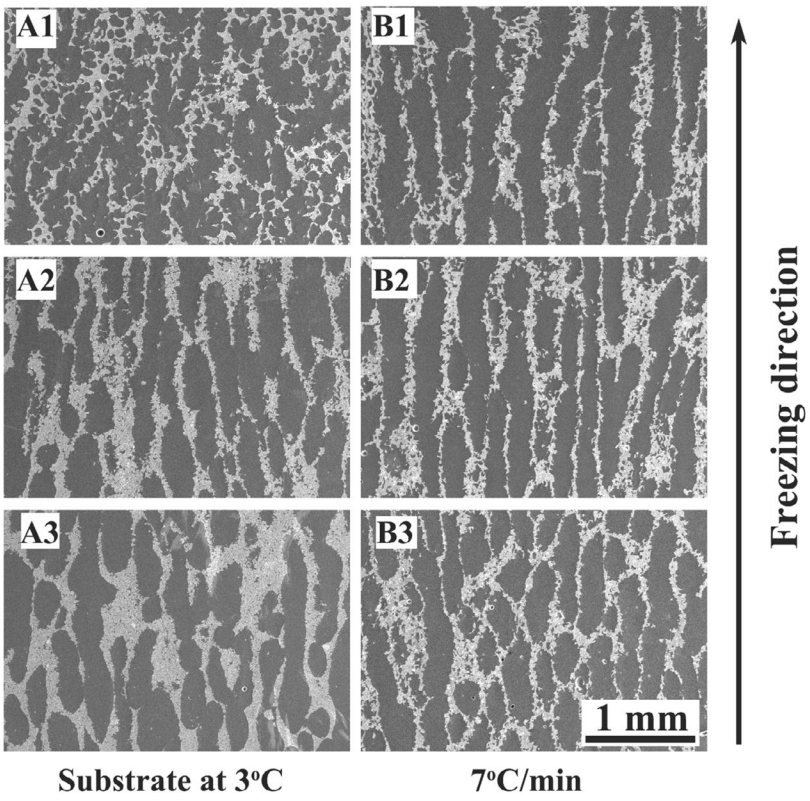

Fig. 5.

SEM images of cross-sections parallel to the freezing direction for constructs after freezing, annealing for 24 h at 34 °C, and sublimation of the camphene. The freezing step was performed on a constant-temperature substrate (3 °C) (A1–A3) or at a constant freezing rate of 7 °C/min (B1–B3). Images are shown for the bottom, middle, and top portions of the constructs along the freezing direction.

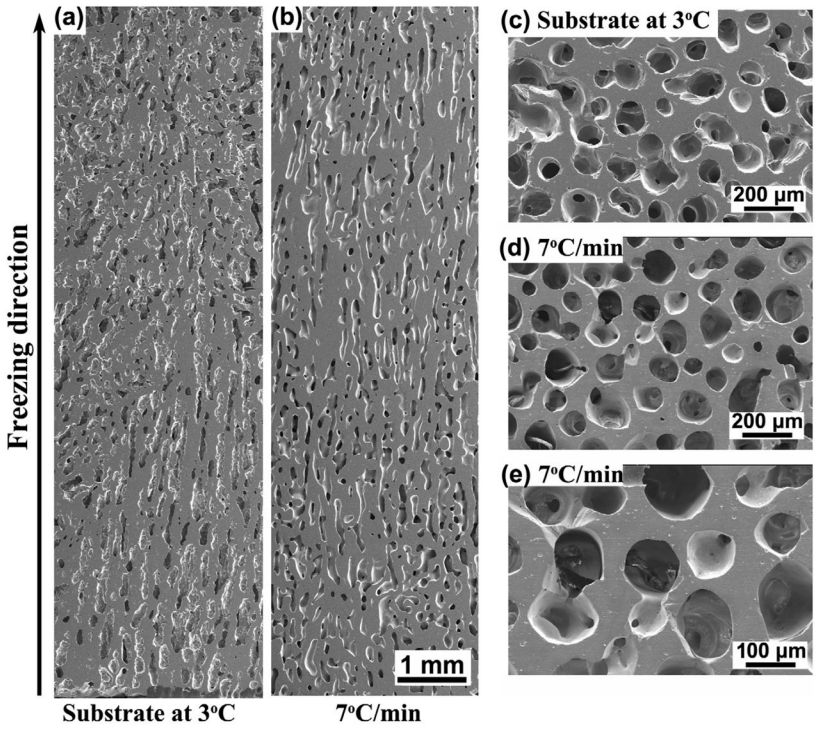

Fig. 6.

SEM images of cross-sections parallel and perpendicular to the freezing direction for sintered constructs (1 h at 700 °C) prepared by freezing on a constant-temperature substrate (3 °C) (a, c), or at a constant rate of 7 °C /min (b, d, e). Sections parallel to the freezing direction (a, b) and perpendicular to the freezing direction (c, d, e) are shown.

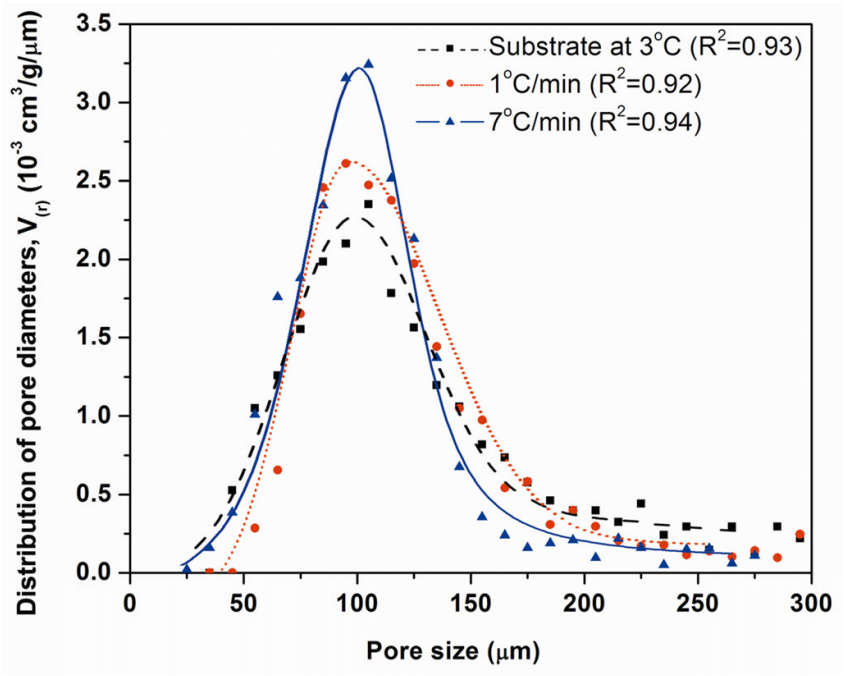

Fig. 7.

Distribution of the pore diameters for sintered constructs (1 h at 700 °C) prepared by freezing on a constant-temperature substrate (3 °C), or at constant freezing rates of 1 and 7°C /min. The data points for each sample were fitted by polynomial function, and the R^2 value for each curve is shown.

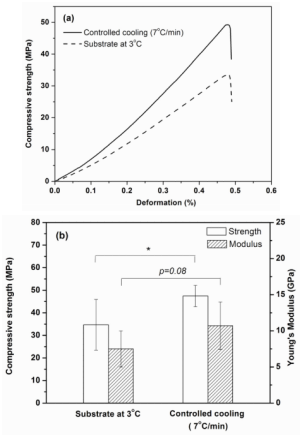

Fig. 8.

(a) Examples of compressive stress vs. deformation response for sintered constructs tested parallel to the orientation direction. The constructs were prepared by freezing on a constant-temperature substrate (3 °C) or at a constant rate of 7 °C /min. (b) Compressive strength and elastic modulus determined from the stress vs. strain data. (*$p < 0.05$)

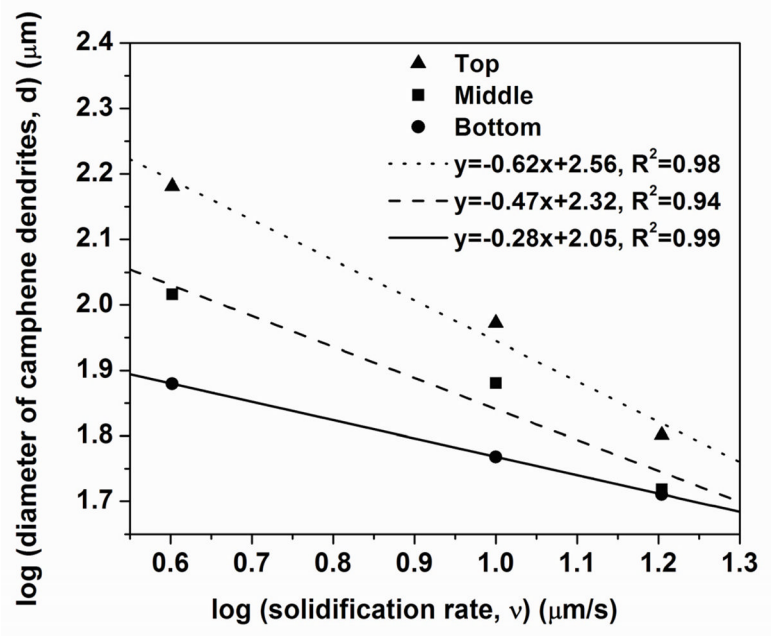

Fig. 9.

Average diameter of primary camphene dendrites vs. average solidification rate for unidirectional freezing of camphene based suspensions at constant rates of freezing. The results are shown for the bottom, middle, and top portions of the construct (total length = 20 mm).